9. Ikawa M, Yamada S, Nakanishi T, Okabe M. Green fluorescent protein (GFP) as a vital marker in mammals. *Curr Top Dev Biol.* 1999;44:1-20.
10. Tabata Y, Ouchi Y, Kamiya H, Manabe T, Arai K, Watanabe S. Retinal fate specification of mouse embryonic stem cells by ectopic expression of Rx/rax, a homeobox gene. *Mol Cell Biol.* 2004;24:4513-4521.
11. Ouchi Y, Tabata Y, Arai K, Watanabe S. Negative regulation of retinal-neurite extension by β-catenin signalling pathway. *J Cell Sci.* 2005;118:4473-4483.
12. Gerdes J, Schwab U, Lemke H, Stein H. Production of a mouse monoclonal antibody reactive with a human nuclear antigen associated with cell proliferation. *Int J Cancer.* 1983;31:13-20.
13. Lendahl U, Zimmerman LB, McKay RD. CNS stem cells express a new class of intermediate filament protein. *Cell.* 1990;60:585-595.
14. Marquardt T, Gruss P. Generating neuronal diversity in the retina: one for nearly all. *Trends Neurosci.* 2002;25:32-38.
15. Takizawa T. 5'-Nucleotidase in rat photoreceptor cells and pigment epithelial cells processed by rapid-freezing enzyme. *J Histochem Cytochem.* 1998;46:1091-1095.
16. Braun N, Brendel P, Zimmerman H. Distribution of 5'-nucleotidase in the developing mouse retina. *Dev Brain Res.* 1995;88:79-86.
17. Watanabe T, Raff MC. Rod photoreceptor development in vitro: intrinsic properties of proliferating neuroepithelial cells change as development proceeds in the rat retina. *Neuron.* 1990;4:461-467.
18. Belliveau MJ, Cepko CL. Extrinsic and intrinsic factors control the genesis of amacrine and cone cells in the rat retina. *Development.* 1999;126:555-566.
19. Yaar R, Jones MR, Chen J-F, Ravid K. Animal models for the study of adenosine receptor function. *J Cell Physiol.* 2005;202:9-20.
20. Yang D, Zhang Y, Nguyen HG, et al. The A2B adenosine receptor protects against inflammation and excessive vascular adhesion. *J Clin Invest.* 2006;116:1913-1923.
21. Kvanta A, Seregard S, Sejersen S, Kull B, Fredholm BB. Localization of adenosine receptor messenger RNAs in the rat eye. *Exp Eye Res.* 1997;65:595-602.
22. Furukawa T, Morrow EM, Li T, Davis FC, Cepko CL. Retinopathy and attenuated circadian entrainment in Crx-deficient mice. *Nat Genet.* 1999;23:466-470.
23. Mears AJ, Kondo M, Swain PK, et al. Nrl is required for rod photoreceptor development. *Nat Genet.* 2001;29:447-452.
24. Burmeister M, Novak J, Liang M-Y, et al. Ocular retardation mouse caused by Chx10 homeobox null allele: impaired retinal progenitor proliferation and bipolar cell differentiation. *Nature.* 1996;12:376-384.
25. Bibb LC, Holt JK, Tarttelin EE, et al. Temporal and spatial expression patterns of the Crx transcription factor and its downstream target: critical differences during human and muse eye development. *Hum Mol Genet.* 2001;15:1571-1579.
26. Akimoto M, Cheng H, Zhu D, et al. Targeting of GFP to newborn rods by Nrl promoter and temporal expression profiling of flow-sorted photoreceptors. *Proc Natl Acad Sci U S A.* 2006;103:3890-3895.
27. Martin PR, Grunert U. Analysis of the short wavelength-sensitive ("Blue") cone mosaic in the primate retina: comparison of new world and old world monkeys. *J Comp Neurol.* 1999;406:1-14.
28. Yoshida S, Mears AJ, Fiedman JS, et al. Expression profiling of the developing and mature Nrl−/− mouse retina: identification of retinal disease candidates and transcriptional regulatory targets of Nrl. *Hum Mol Genet.* 2004;13:1487-1503.
29. Kennan A, Aherne A, Palfi A, et al. Identification of an IMPDH1 mutation in autosomal dominant retinitis pigmentosa (RP10) revealed following comparative microarray analysis of transcripts derived from retinas of wild-type and Rho (−/−) mice. *Hum Mol Genet.* 2002;11:547-557.
30. Kreutzberg GW, Hussain ST. Cytochemical heterogeneity of the glial plasma membrane: 5'-nucleotidase in retinal Muller cells. *J Neurocytol.* 1982;11:53-64.
31. Kreutzberg GW, Hussain ST. Cytochemical localization of 5'-nucleotidase activity in retinal photoreceptor cells. *Neuroscience.* 1984;11:857-866.
32. Furukawa T, Morrow EM, Cepko CL. Crx, a novel otx-like homeobox gene, shows photoreceptor-specific expression and regulates photoreceptor differentiation. *Cell.* 1997;91:531-541.
33. Spychala J, Kitajewski J. Wnt and beta-catenin signaling target the expression of ecto-5'-nucleotidase and increase extracellular adenosine generation. *Exp Cell Res.* 2004;296:99-108.
34. Synnestvedt K, Furuta GT, Comerford KM, et al. Ecto-5'-nucleotidase (CD73) regulation by hypoxia-inducible factor-a mediates permeability changes in intestinal epithelia. *J Clin Invest.* 2002;110:993-1002.
35. Chen S, Wang QL, Nie Z, et al. Crx, a novel Otx-like paired-homeodomain protein, binds to and transactivates photoreceptor cell-specific genes. *Neuron.* 1997;19:1017-1030.

Nongenetic method for purifying stem cell–derived cardiomyocytes

Fumiyuki Hattori[1,2], Hao Chen[1,3], Hiromi Yamashita[1], Shugo Tohyama[1,3], Yu-suke Satoh[1,4], Shinsuke Yuasa[1], Weizhen Li[1], Hiroyuki Yamakawa[1,3], Tomofumi Tanaka[1,2], Takeshi Onitsuka[1,3], Kenichiro Shimoji[1,3], Yohei Ohno[1,3], Toru Egashira[1,3], Ruri Kaneda[1], Mitsushige Murata[1,3], Kyoko Hidaka[5], Takayuki Morisaki[5], Erika Sasaki[6], Takeshi Suzuki[4], Motoaki Sano[1], Shinji Makino[1], Shinzo Oikawa[2] & Keiichi Fukuda[1]

Several applications of pluripotent stem cell (PSC)-derived cardiomyocytes require elimination of undifferentiated cells. A major limitation for cardiomyocyte purification is the lack of easy and specific cell marking techniques. We found that a fluorescent dye that labels mitochondria, tetramethylrhodamine methyl ester perchlorate, could be used to selectively mark embryonic and neonatal rat cardiomyocytes, as well as mouse, marmoset and human PSC-derived cardiomyocytes, and that the cells could subsequently be enriched (>99% purity) by fluorescence-activated cell sorting. Purified cardiomyocytes transplanted into testes did not induce teratoma formation. Moreover, aggregate formation of PSC-derived cardiomyocytes through homophilic cell-cell adhesion improved their survival in the immunodeficient mouse heart. Our approaches will aid in the future success of using PSC-derived cardiomyocytes for basic and clinical applications.

Human embryonic stem cells (ESCs) and induced pluripotent stem cells (iPSCs) could prove to be an unlimited source of cardiomyocytes. Several studies have achieved directed differentiation of mouse, monkey and human ESCs into cardiomyocytes[1–3] but with variable efficiency. Some protocols describe up to 60% differentiation efficiency, but none achieve >99% of cells differentiating into cardiomyocytes without the use of genetic selection methods[4]. Transplantation of undifferentiated ESCs results in the formation of teratomas[5]. Thus, it is necessary to purify ESC-derived cardiomyocytes before transplantation.

ESC lines with various combinations of cardiomyocyte-specific reporters can be used to obtain highly pure ESC-derived cardiomyocytes[4,6–10], but this requires genetic modification of the cells. Also, discontinuous Percoll density gradient centrifugation could be used to enrich for mouse and human ESC-derived cardiomyocytes, but the purity of the cardiomyocytes in these preparations is relatively low[11,12]. Here we show that cardiomyocytes in early mouse embryos or those differentiated from pluripotent stem cells (PSCs) have high mitochondrial content and can be purified without the need for genetic modification, using fluorescent dyes that label mitochondria.

RESULTS

Characterization of mitochondrial dyes

In primary cultures of neonatal rat heart cells stained with MitoTracker Red (Invitrogen) the fluorescence intensity of cardiomyocytes was much higher compared to that of nonmyocytes (**Fig. 1a**). MitoTracker Red and tetramethylrhodamine methyl ester perchlorate (TMRM) specifically accumulated in both the subsarcomeric mitochondria, located around the nucleus and in the intermyofibrillar mitochondria (**Fig. 1a** and **Supplementary Fig. 1**). To confirm specific mitochondrial staining of MitoTracker dyes, we stained neonatal rat cardiomyocytes with MitoTracker Red and JC-1 (a mitochondrial voltage-sensitive dye; **Supplementary Fig. 2**).

Fluorescence-activated cell sorter (FACS) analysis of cells dissociated from neonatal heart revealed three main populations (**Fig. 1b**). We sorted the populations with the highest (designated as fraction 1), the middle (fraction 2) and the lowest (fraction 3) fluorescence intensity and cultured them separately. All the cells in fraction 1 showed rhythmic beating and were immunostained with an antibody to α-actinin (**Fig. 1c**), indicating they were cardiomyocytes. We identified very few cardiomyocytes in fraction 2 (**Fig. 1c**). Fraction 3 consisted of red blood cells and dead cells. We confirmed the neonatal rat cardiomyocyte content in fraction 1 by immunofluorescence staining for α-actinin to be 99.4 ± 0.6% (**Fig. 1d**), and the yield was approximately 5×10^5 cells from a single heart.

Next, we compared the efficacy of various mitochondrial dyes for separating the neonatal rat cardiomyocyte population from the nonmyocytes and found that TMRM was the most effective (**Fig. 1e,f**). We then evaluated the washout efficiencies of the dyes and found that TMRM disappeared completely within 24 h, whereas

[1]Department of Regenerative Medicine and Advanced Cardiac Therapeutics, Keio University School of Medicine, Tokyo, Japan. [2]Asubio Pharma Co., Ltd., Osaka, Japan. [3]Division of Cardiology, Department of Medicine, Keio University School of Medicine, Tokyo, Japan. [4]Division of Basic Biological Sciences, Faculty of Pharmacy, Keio University, Tokyo, Japan. [5]Department of Bioscience, National Cardiovascular Center Research Institute, Osaka, Japan. [6]Laboratory of Applied Developmental Biology, Marmoset Research Department, Central Institute for Experimental Animals, Kanagawa, Japan. Correspondence should be addressed to K.F. (kfukuda@sc.itc.keio.ac.jp).

RECEIVED 10 AUGUST; ACCEPTED 15 OCTOBER; PUBLISHED ONLINE 29 NOVEMBER 2009; DOI:10.1038/NMETH.1403

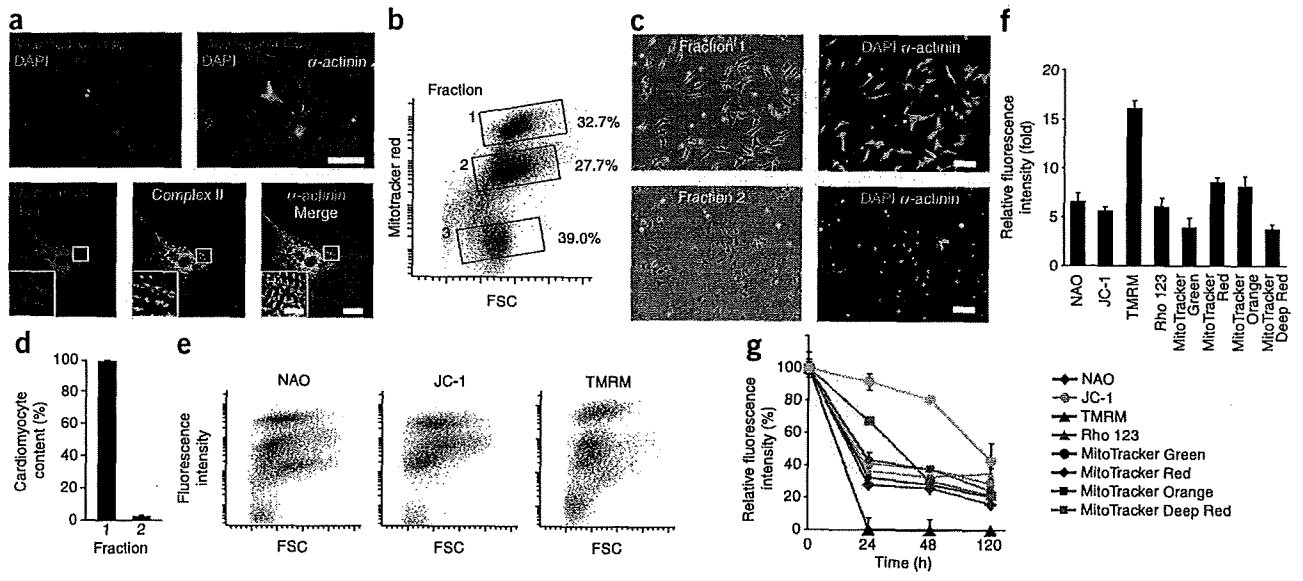

Figure 1 | *Mitochondrial dyes for cardiomyocyte purification.* (**a**) *Fluorescence images of neonatal rat cardiomyocytes prestained with MitoTracker Red* and immunostained for α-actinin (top) or prestained with MitoTracker Red and immunostained for mitochondrial electron transfer chain complex II (complex II) and α-actinin (bottom). DAPI, nuclear stain. Scale bars, 100 μm (top); 20 μm (bottom); and 10 μm (bottom inset). (**b**) FACS analysis of neonatal rat heart-derived cells stained with MitoTracker Red. The sorted cells were divided into fractions 1–3 (boxed). FSC, forward scatter. (**c**) Immunofluorescence staining for α-actinin of cells from fractions 1 and 2. Blue, DAPI staining. Scale bars, 100 μm. (**d**) Cardiomyocyte content in fractions 1 and 2. Data are shown as mean ± s.d. (n = 3). (**e**) Representative FACS plots of dissociated cells from neonatal rat heart stained with mitochondrial dyes. (**f**) Relative fluorescence intensity of the indicated mitochondrial dyes in fractions 1 versus 2. Data are shown as mean ± s.d. (n = 3). (**g**) Washout of the indicated mitochondrial dyes from neonatal rat cardiomyocytes. Data are shown as mean ± s.d. (n = 3).

other dyes remained for at least 5 d (**Fig. 1g** and **Supplementary Fig. 3a**). TMRM and JC-1 at 100 nM did not affect cell viability using 3-(4,5-dimethyl-thiazol-2-yl)-2,5-diphenyltetrazolium bromide (MTT) assay, whereas other dyes affected viability differently (**Supplementary Fig. 3b**). Based on these results, we selected TMRM for subsequent experiments.

Purification of cardiomyocytes from heart and whole embryos

To investigate the mitochondrial content of cardiomyocytes at different developmental stages, we performed FACS analysis of rat hearts at embryonic day 11.5 (E11.5) to postnatal day 8 (P8); the hearts had been dissociated and labeled with TMRM (**Fig. 2a**). The mean ratio of TMRM fluorescence in fraction 1 to fraction 2 gradually increased with increasing embryonic stage and rapidly after birth (**Fig. 2b**). FACS analysis followed by immunofluorescence staining confirmed over 99% cardiomyocyte purity at all stages (**Fig. 2c,d**).

We then stained live embryos (E11.5 and E12.5) with TMRM. The heart showed markedly stronger fluorescence compared with other tissues (**Fig. 2e** and **Supplementary Video 1**). Intraplacental injection of MitoTracker Red also resulted in the strongest accumulation of fluorescence in the heart via embryonic circulation. However, other tissues had much weaker fluorescence (**Supplementary Fig. 4**).

To assess why there was strong TMRM fluorescence in the embryonic heart, we compared expression levels of complex I–V of the 36 kDa mitochondrial outer membrane protein porin (also known as the voltage-dependent anion channel) and of heat shock protein 70 between cardiac and various noncardiac tissues in rat E12.5 embryos; we detected markedly stronger expression in the myocardium (**Supplementary Fig. 5**). Furthermore, immunostaining of the fetal heart area for α-actinin, manganese superoxide dismutase (MnSOD) and platelet endothelial cell adhesion molecule (PECAM) (markers of cardiomyocytes, mitochondria and the endothelium, respectively), revealed that MnSOD immunostaining overlapped that for α-actinin but not for PECAM (**Fig. 2f**). Taken together, the accumulation of fluorescent dyes that label mitochondria may reflect high mitochondria abundance in the heart.

Next, we treated dissociated cells obtained from E11.5 to E13.5 whole rat embryos with TMRM and analyzed them on a FACS (**Fig. 2g**). Some cells in this preparation were autofluorescent, which was due to the presence of lipopigments and flavins[13]. To obtain only TMRM-fluorescent cells and eliminate contamination by autofluorescent cells, we adopted pseudo-two-dimensional separation (**Fig. 2g** and Online Methods). We isolated populations with the highest TMRM-fluorescence from dispersed cells of E11.5, E12.5 and E13.5 whole rat embryos. The sorted cells from E11.5 embryos were immunostained for α-actinin (purity 99%, n = 3 embryos; yield, ~5 × 10^3 cells per embryo). We obtained similar results with E12.5 and E13.5 embryos. At these embryonic stages (E11.5–E13.5), the embryos contain skeletal myoblasts only and not mature myotubes. We found that mature skeletal myotubes, which could not pass through the FACS, could be marked with TMRM, whereas skeletal myoblasts, which do pass through the FACS, were not marked by TMRM (**Supplementary Fig. 6**).

Purification of PSC-derived cardiomyocytes

We first observed cardiomyocytes differentiated from mouse ESCs on day 7 of differentiation; the cells had marked TMRM accumulation. After TMRM staining, we fixed the cells and immunostained them for Nkx2.5 and α-actinin (**Fig. 3a**). The Nkx2.5– and α-actinin–positive areas and TMRM-positive area in the mouse

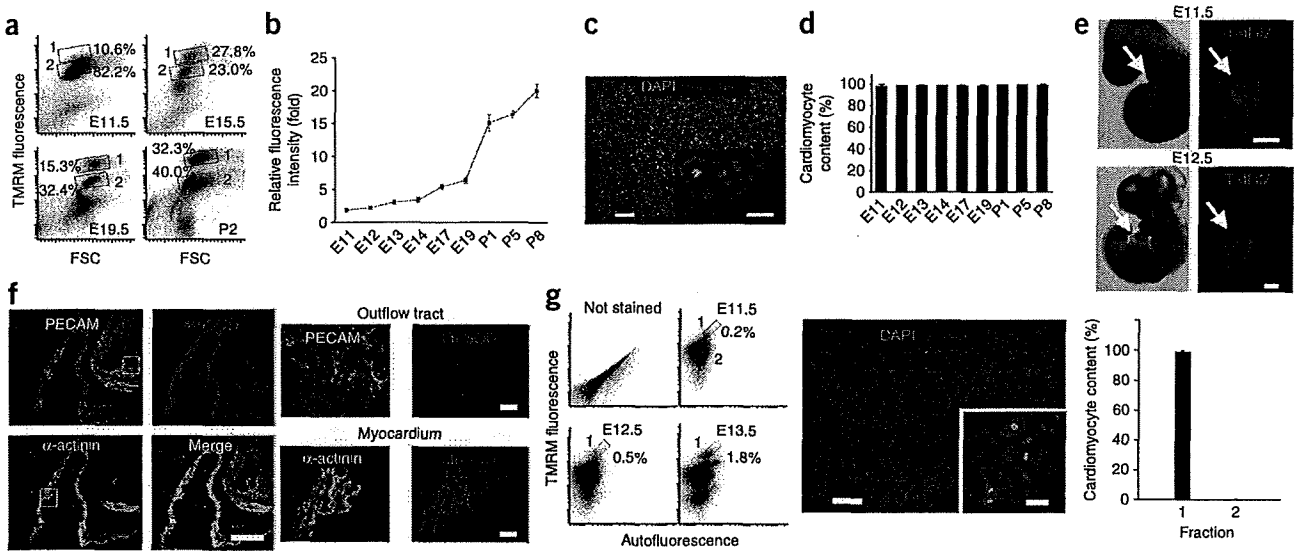

Figure 2 | Purification of cardiomyocytes from embryonic heart and whole embryo. (**a**) Representative FACS analysis of TMRM-stained rat embryonic heart cells at the indicated ages. Fractions 1 and 2 were typical gates for cardiomyocytes and noncardiomyocytes, respectively. (**b**) Relative fluorescence intensity of fraction 1 versus fraction 2 in the developing rat heart. Data are shown as mean ± s.d. ($n = 3$). (**c**) Immunofluorescence staining for α-actinin in the fraction 1 gated cells from E11.5 rat heart. (**d**) Cardiomyocyte content of the fraction 1-gated cells obtained from E11.5–P8 rat hearts. Data are shown as mean ± s.d. ($n = 3$). (**e**) Bright field (left) and fluorescence (right) images of whole rat embryos of indicated ages. (**f**) Immunofluorescence staining of rat E11.5 embryo for the indicated markers, PECAM, α-actinin and MnSOD. Images show pericardiac area (left four) and magnification of the boxed areas is shown on the right. (**g**) FACS analysis (left) of dissociated cells from whole embryos in the absence (not stained) or presence of TMRM at the indicated stages. Boxes indicate fractions 1 and 2; percentages of fraction 1 cells are shown. Immunofluorescence staining (middle) for α-actinin in the cells obtained from fraction 1 of E11.5 embryos. Cardiomyocyte content of fractions 1 and 2 at E11.5 is shown (right). Data are shown as mean ± s.d. ($n = 3$). Scale bars, 100 μm (**c**,**g**,**e**); 200 μm (**f** left); and 20 μm (**c** inset, **f** right, **g** inset).

ESC–derived cardiomyocytes were colocalized completely, although the intracellular localization of TMRM, Nkx2.5 and α-actinin was clearly different. Notably, TMRM dissociated rapidly into the bulk solution compared with other dyes upon fixation (**Supplementary Fig. 7**), indicating that there is likely to be no effect of TMRM on subsequent immunohistochemical analysis.

We applied pseudo–two-dimensional FACS analysis to the embryoid body–derived cells (**Fig. 3b**). We first observed fraction 1 cells 7 d after embryoid body formation. Both the ratio of the mean TMRM fluorescence in fraction 1 (cardiomyocytes) to fraction 2 (noncardiomyocytes) and the percentage of cells in fraction 1 increased gradually until day 15 (**Fig. 3c,d**), suggesting that the best time for obtaining mouse ESC–derived cardiomyocytes was at day 15.

We sorted approximately 5×10^5 to 9×10^5 cells from day 15 embryoid bodies. The viability of the sorted cells was 99.1 ± 1.5%, as confirmed by trypan blue staining (**Supplementary Fig. 8**). This high viability may be due to the fact that the cells were sorted based on TMRM accumulation (and thus contained active mitochondria). We cultured the sorted cells for 7 d to allow the cells to attach to the substrate and to elongate (Online Methods). Immunofluorescence staining for α-actinin and Nkx2.5 in three independent experiments confirmed that these cells were high-purity cardiomyocytes (99.5 ± 0.3%; **Fig. 3e**). We obtained >99% pure ESC-derived cardiomyocytes from day 12–25 embryoid bodies (**Fig. 3f**). We also obtained highly pure cardiomyocytes from mouse iPSCs (**Fig. 3g,h**).

To investigate the possibility of isolating cardiac progenitor cells, we stained whole E7.5 and E7.75 embryos. We found that TMRM faintly, but distinctly, marked the cardiac crescent, which contains cardiomyogenic precursor cells, indicating a possible applicability of our method to obtaining progenitor cells. Next, we carried out time-lapse fluorescence microscopy on attached mouse embryoid bodies stained with TMRM (**Supplementary Fig. 9**). We first observed TMRM-positive cells on day 6.5. Fluorescence in these cells increased gradually between days 6.5 and 7 and they started beating on day 7.0. In contrast, TMRM-negative cells did not beat during the experiments. We then performed FACS analysis on dissociated cells obtained from day 3–6.5 embryoid bodies and stained with TMRM. There were no cells in fraction 1. The higher TMRM-fluorescence cells in fraction 2 from day 3 and 4 embryoid bodies did not differentiate into cardiomyocytes, even after subsequent culture of attached cells for up to 8 d. In the case of day 6.5 embryoid bodies, some of the isolated cells differentiated into cardiomyocytes upon subsequent culture for 3 d. We also stained *Nkx2.5-GFP* knock-in mouse ESCs[6], which we and others have used frequently to isolate cardiomyocytes. After embryoid body formation, we first observed GFP fluorescence on day 7, whereas we observed TMRM staining on day 6.5 (**Supplementary Fig. 10**). Our observations indicate that our method can be used to purify differentiated cardiomyocytes but not cardiac progenitor cells.

We differentiated common marmoset ESCs, human ESCs and human iPSCs into cardiomyocyte-containing embryoid bodies by conventional floating cell culture. We transferred the embryoid bodies into the cell-attachment dishes with 10 nM TMRM. Beating embryoid bodies had extremely high TMRM fluorescence compared with that of nonbeating embryoid bodies derived from marmoset and human ESCs (**Fig. 4a**). Then we dispersed embryoid body–derived cells, stained them with TMRM and analyzed them on a FACS (**Fig. 4b**). We fixed sorted human

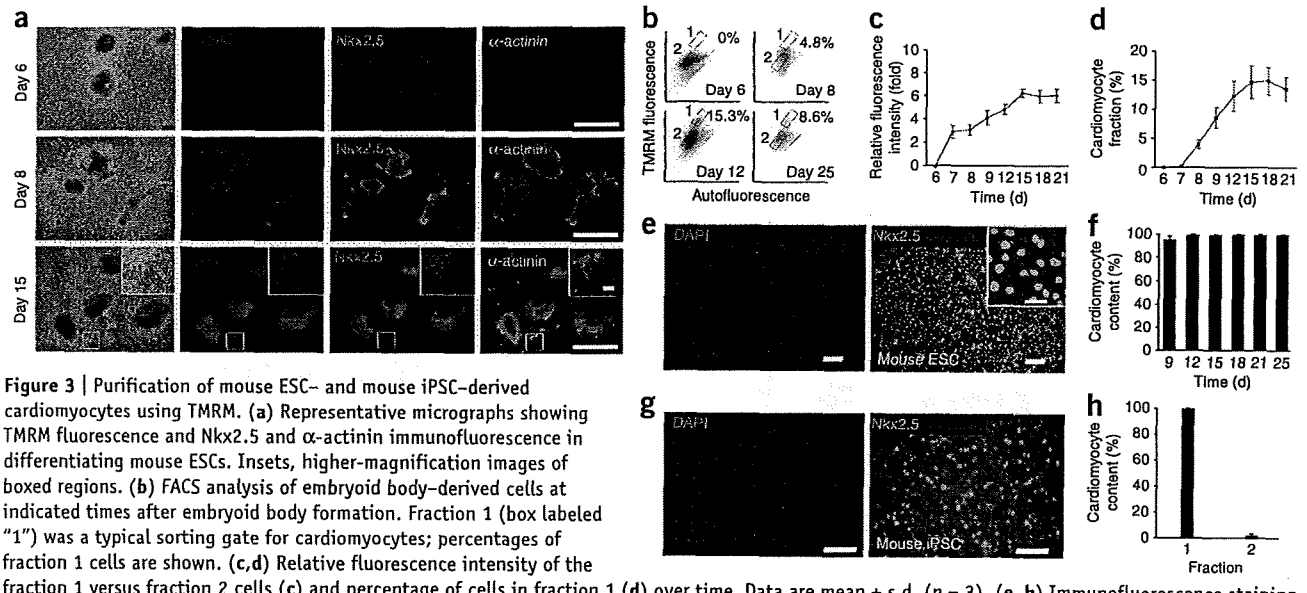

Figure 3 | Purification of mouse ESC- and mouse iPSC-derived cardiomyocytes using TMRM. (**a**) Representative micrographs showing TMRM fluorescence and Nkx2.5 and α-actinin immunofluorescence in differentiating mouse ESCs. Insets, higher-magnification images of boxed regions. (**b**) FACS analysis of embryoid body-derived cells at indicated times after embryoid body formation. Fraction 1 (box labeled "1") was a typical sorting gate for cardiomyocytes; percentages of fraction 1 cells are shown. (**c**,**d**) Relative fluorescence intensity of the fraction 1 versus fraction 2 cells (**c**) and percentage of cells in fraction 1 (**d**) over time. Data are mean ± s.d. ($n = 3$). (**e**–**h**) Immunofluorescence staining for Nkx2.5 and α-actinin in cultured fraction 1 cells sorted from day 15 embryoid bodies differentiated from mouse ESCs (**e**) and from mouse iPSCs (**g**); and cardiomyocyte content in cultured cells sorted from day 9–25 embryoid bodies differentiated from mouse ESCs (**f**) and in cultured cells sorted from day 15 embryoid bodies differentiated from mouse iPSCs (**h**). Data are mean ± s.d. ($n = 3$). Scale bars, 1 mm (**a**); and 100 μm (**a** inset, **e**,**g**).

cells in fraction 1, immunostained them for Nkx2.5 and subjected them to a second FACS analysis. The results showed that over 99.9% of cells in fraction 1 were cardiomyocytes (**Fig. 4c**). Furthermore, we compared expression of cardiac and noncardiac genes in human ESC–derived cardiomyocytes isolated by our method and in unpurified cells from embryoid bodies using real-time PCR. We observed a marked increase in the expression of myocardial genes and a decrease in the expression of nonmyocardial genes in purified human ESC–derived cardiomyocytes (**Supplementary Fig. 11**).

We also cultured the sorted cells for 5 d and immunostained them for Nkx2.5 and α-actinin (**Fig. 4d**). Common marmoset ESC, human ESC and human iPSC fraction 1 comprised 99.0 ± 1.0%, 99.0 ± 0.9% and 99.3 ± 0.2% cardiomyocytes, respectively; in contrast, fraction 2 had 2.3 ± 0.6%, 2.5 ± 0.2% and 1.7 ± 1.6% cardiomyocytes, respectively (**Fig. 4e**). To estimate the acquisition efficiency in the sorting experiments, we compared by FACS analysis the cardiomyocyte fraction obtained by TMRM with that obtained by immunofluorescence staining for α-actinin. The number of cardiomyocytes isolated by TMRM staining was 60–90% of the number defined by α-actinin staining (**Supplementary Fig. 12**). To rule out the possibility of skeletal muscle contamination in the sorted cardiomyocyte population, we extracted total mRNA from sorted cardiomyocytes and evaluated it for *myoD* expression using real-time PCR. We confirmed that there was no amplification of *myoD* (**Supplementary Fig. 13**).

No teratoma formation

We cultured the purified mouse ESC-derived cardiomyocytes and noncardiomyocytes for 7 d and found that although noncardiomyocytes formed piled-up colonies, in which some cells

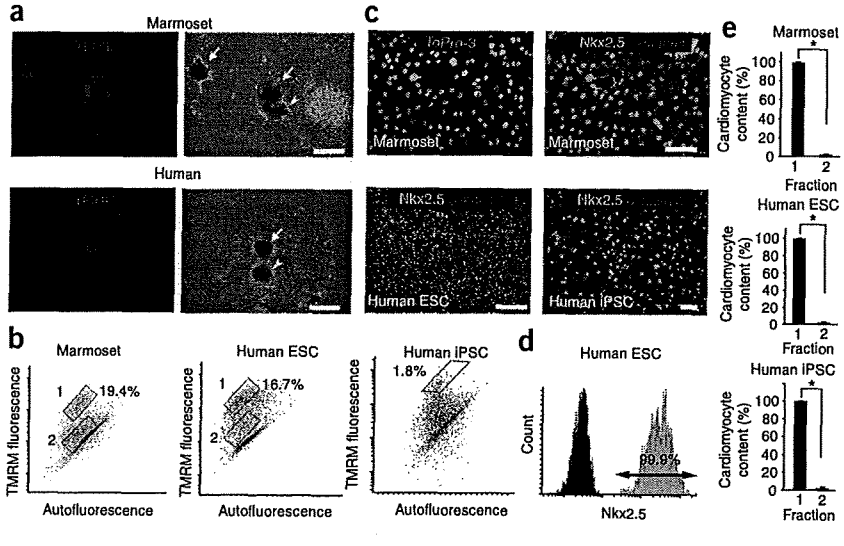

Figure 4 | Purification of PSC-derived cardiomyocytes in human and marmoset. (**a**) TMRM fluorescence (left) and phase contrast (right) images of marmoset and human embryoid bodies containing beating cardiomyocytes. Arrows, beating areas; arrowheads, nonbeating areas. (**b**) FACS separation of TMRM-stained cardiomyocytes derived from common marmoset ESCs, human ESCs and human iPSCs. Fractions 1 and 2 are boxed; percentages of fraction 1 cells are shown. (**c**) Immunofluorescence staining of fraction 1 cells for α-actinin and Nkx2.5. ToPro-3 represents nuclear staining. (**d**) Histogram showing immunodetection of Nkx2.5 (gray) and negative control (without first antibody; black) in sorted human ESC-derived fraction 1 cells. (**e**) The cardiomyocyte content of fractions 1 and 2 in common marmoset ESCs, human ESCs and human iPSCs. Data are mean ± s.d. ($n = 3$). *$P < 0.01$ (Student *t*-test). Scale bars, 500 μm (**a**); and 100 μm (**c**).

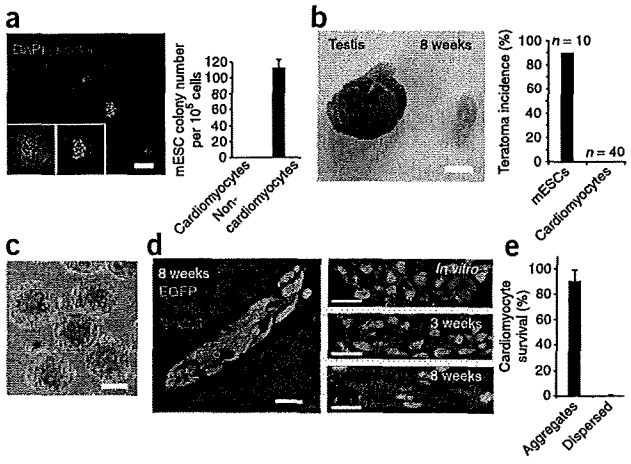

Figure 5 | Transplantation of purified mouse ESC-derived cardiomyocytes. (**a**) Immunofluorescence staining for Oct3/4 (red) in the sorted cells from the noncardiac fraction (left), and numbers of mouse ESC-like colonies obtained from 10^5 sorted cells (right). Data are mean ± s.d. ($n = 3$). (**b**) Transplantation of 250 undifferentiated mouse ESCs into testes resulted in teratoma formation (testis), whereas transplantation of 1.9×10^5 purified mouse ESC-derived cardiomyocytes did not (8 weeks). Incidence of teratoma formation was quantified (right). (**c**) Phase contrast image of mouse cardiomyocyte aggregates. (**d**) Immunofluorescence staining of engrafted mouse cardiomyocyte aggregates for α-actinin and Nkx2.5 8 weeks after transplantation (left); transplanted cells expressed EGFP. Mouse ESC-derived cardiomyocytes *in vitro* and 3 and 8 weeks after transplantation immunostained for Nkx2.5 and α-actinin (right). (**e**) Transplanted mouse ESC-derived cardiomyocyte survival. Data are shown as mean ± s.d. ($n = 5$). Scale bars, 100 μm (**a**,**c**); 5 mm (**b**); and 20 μm (**d**).

were positive for Oct3/4, the cardiomyocytes did not (**Fig. 5a**). Further, we transplanted 1.9×10^5 aggregated mouse ESC–derived cardiomyocytes and 250 undifferentiated mouse ESCs as a control into the testes of immunocompromised nonobese diabetic–severe combined immunodeficient (NOD-SCID) mice. Two months later, 90% of the control mice developed teratomas (9 of 10 mice), but we did not detect teratomas in any of the mice transplanted with purified mouse ESC–derived cardiomyocytes (0 of 40 mice) (**Fig. 5b**). We tried to verify that there was no teratoma formation in the heart by directly injecting mouse ESC–derived cardiomyocytes (1×10^5) into the myocardium of five NOD-SCID mice immediately after sorting. Two months later, we found few (<1%) of the transplanted cardiomyocytes in the heart (data not shown).

To understand the mechanism underlying this cell loss, we injected purified and MitoTracker Red–labeled neonatal rat cardiomyocytes into the left ventricular free wall of *ex vivo*–perfused hearts. We found one-third to one-half of injected cells in the postperfusion solution, indicating that the neonatal rat cardiomyocytes were washed out within the first 10 min (**Supplementary Fig. 14**). Next, we compared the tissue adhesiveness of purified mouse ESC–derived cardiomyocytes and mouse embryonic fibroblasts (MEFs) by counting cells in continuous sections of whole ventricles 24 h after injection into the left ventricular free walls. We found that less than 1% of the grafted ESC-derived cardiomyocytes had adhered to the host myocardium, compared with 50% of MEFs.

Transplantation of PSC-derived cardiomyocytes

From the above observations, we reasoned that loss of transplanted ESC-derived cardiomyocytes may be due to rapid washout and low adhesiveness of the cells. Because ESC-derived cardiomyocytes existed as homophilic cell aggregates (diameter, 100–500 μm) in mouse, marmoset and human embryoid bodies (**Supplementary Fig. 15**), we suspected that re-aggregated purified ESC-derived cardiomyocytes may be more resistant to rapid washout. We generated cardiomyocyte aggregates by seeding 313–10,000 purified mouse ESC–derived cardiomyocytes onto nonadhesive 96-well plates. One day after seeding, the cells adhered to each other, aggregated and started synchronized beating; 5 d later, cardiomyocyte aggregates formed with diameters of 100–450 μm (**Fig. 5c**, **Supplementary Fig. 16** and **Supplementary Video 2**). Propidium iodide staining revealed that a high proportion of re-aggregated mouse ESC–derived cardiomyocytes were viable (98.8 ± 0.2% of seeded cells; **Supplementary Fig. 16**).

We transplanted mouse cardiomyocyte aggregates into the ventricular free walls of NOD-SCID mice and killed the mice at 3 and 8 weeks ($n = 5$ for both groups). We observed no teratoma formation in either group. Immunofluorescence staining revealed that cell aggregates positive for the tracers Nkx2.5 and α-actinin were located in the left ventricle (**Fig. 5d**). The number of cells that survived in the heart was greater than 90% (**Fig. 5e**). Furthermore, we repeated these experimental procedures using purified human ESC–derived cardiomyocytes (**Supplementary Video 3**). Two months after transplantation, we detected a large amount of human myocardial tissue in NOD-SCID mouse heart (**Supplementary Fig. 17**).

Finally, we investigated which autoparacrine factors are important for the survival of ESC-derived cardiomyocytes. Human cardiomyocyte aggregates remained viable under serum-free culture conditions; moreover, their diameters increased by approximately twofold by day 25. Supplementation of the cultures with physiological concentrations of basic fibroblast growth factor (bFGF), epidermal growth factor (EGF), platelet-derived growth factor beta dimer (PDGF-BB) and endothelin-1 (ET-1) strongly enhanced the growth of the cardiomyocyte aggregates (**Supplementary Fig. 18a** and **Supplementary Video 4**). We confirmed expression of these growth factors and their receptors by real-time PCR (probe and primer sets are listed in **Supplementary Table 1**). We also confirmed that these growth factors were expressed in adult human and mouse hearts (**Supplementary Fig. 18b**). Autoparacrine stimulation with these growth factors may be one reason why grafted cardiomyocyte aggregates survived and grew in the host myocardium.

DISCUSSION

Our method for cardiomyocyte isolation has two advantages. First, it does not require genetic modification of the cells. Genetic modifications using nonviral or viral systems have several disadvantages: extrinsic genes may be silenced, the number of integration events in one cell is difficult to control, targeted integration is not straightforward, and line selection as well as verification of proper expression of extrinsic genes[14] is time-consuming. Furthermore, genetic modification carries risks such as possible tumor formation[15–17]. Second, our method is likely to be widely applicable. We demonstrated that it may be used to purify ESC-derived cardiomyocytes in four species, including human,

and that it is also applicable to mouse and human iPSCs. High abundance of cellular mitochondria is likely to be a common characteristic of cardiomyocytes irrespective of species. In contrast, most genetic modifications require species-specific constructs. Our simple purification strategy should facilitate basic studies using embryonic heart and stem cell–derived cardiomyocytes; furthermore, this strategy can also allow isolation of noncardiomyocytes, which may open up new approaches to studying developmental interactions.

The ESC-derived cardiomyocytes purified using our method did not induce teratoma formation in either the heart or testes. Although from the viewpoint of clinical safety, further studies using large animal models with a much larger number of ESC-derived cardiomyocytes will be required, we believe that our purification method may have considerable advantages over existing methods for eventual clinical translation as well.

Our results suggest that induction of mitochondrial biogenesis begins shortly before beating of cardiomyocytes. This indicates the tight relationship between cardiomyogenesis and mitochondrial biogenesis. A combination of our strategy and other marking techniques for cardiac progenitor cells may facilitate study in this field.

Unpurified fetal and neonatal rat cardiomyocytes and bone marrow mesenchymal and ESC-derived cardiomyocytes have been shown to survive in the recipient heart[18–20]. In contrast, purified and dispersed cardiomyocytes differentiated from ESCs did not achieve a high survival rate[5]. Re-aggregation augmented the long-term survival of purified mouse and human ESC–derived cardiomyocytes. Our results indicate that ESC-derived cardiomyocytes might be highly anchorage-dependent, and that homophilic cell-to-cell adhesion and autoparacrine signaling may be important factors contributing to their survival.

METHODS

Methods and any associated references are available in the online version of the paper at http://www.nature.com/naturemethods/.

Note: Supplementary information is available on the Nature Methods website.

ACKNOWLEDGMENTS

Human ESCs were a gift of N. Nakatsuji at the Department of Development and Differentiation, Institute for Frontier Medical Sciences, Kyoto University. Human and mouse iPSCs were a gift of S. Yamanaka at the Center for iPS Cell Research and Application, Institute for Integrated Cell-Material Sciences, Kyoto University. Mouse ESCs were a gift of H. Niwa at the Laboratory of Pluripotent Cell Studies, RIKEN Center for Developmental Biology. This study was supported in part by research grants from the Ministry of Education, Science and Culture, Japan, and by the Program for Promotion of Fundamental Studies in Health Science of the National Institute of Biomedical Innovation.

AUTHOR CONTRIBUTIONS

F.H. designed the whole study. F.H. performed most experiments and wrote the manuscript. H.C. participated in cell-sorting experiments and prepared cells. H.Yamashita participated in cell-sorting experiments, PCR experiments, immunofluorescent staining, animal experiments and preparing cells. S.T., Y.S., W.L., T.T., T.O., K.S., Y.O. and T.E. participated in cell preparations. H.Yamakawa and M.M. participated in heart perfusion experiments. K.H. and T.M. provided the *Nkx2.5 knock-in* ESCs. S.Y., M.M., R.K., M.S., S.M. and S.O. provided advice. E.S. provided cmESCs. T.S. supervised Y.S. K.F. provided advice, obtained the budget and supervised the project.

COMPETING INTERESTS STATEMENT

The authors declare competing financial interests: details accompany the full-text HTML version of the paper at http://www.nature.com/naturemethods/.

Published online at http://www.nature.com/naturemethods/.
Reprints and permissions information is available online at http://npg.nature.com/reprintsandpermissions/.

1. Yuasa, S. *et al.* Transient inhibition of BMP signaling by Noggin induces cardiomyocyte differentiation of mouse embryonic stem cells. *Nat. Biotechnol.* **23**, 607–611 (2005).
2. Nemir, M., Croquelois, A., Pedrazzini, T. & Radtke, F. Induction of cardiogenesis in embryonic stem cells via downregulation of Notch1 signaling. *Circ. Res.* **98**, 1471–1478 (2006).
3. Mummery, C. *et al.* Differentiation of human embryonic stem cells to cardiomyocytes: role of coculture with visceral endoderm-like cells. *Circulation* **107**, 2733–2740 (2003).
4. Anderson, D. *et al.* Transgenic enrichment of cardiomyocytes from human embryonic stem cells. *Mol. Ther.* **15**, 2027–2036 (2007).
5. Kolossov, E. *et al.* Engraftment of engineered ES cell-derived cardiomyocytes but not BM cells restores contractile function to the infarcted myocardium. *J. Exp. Med.* **203**, 2315–2327 (2006).
6. Hidaka, K. *et al.* Chamber-specific differentiation of Nkx2.5-positive cardiac precursor cells from murine embryonic stem cells. *FASEB J.* **17**, 740–742 (2003).
7. Fijnvandraat, A.C. *et al.* Cardiomyocytes purified from differentiated embryonic stem cells exhibit characteristics of early chamber myocardium. *J. Mol. Cell. Cardiol.* **35**, 1461–1472 (2003).
8. Gassanov, N., Er, F., Zagidullin, N. & Hoppe, U.C. Endothelin induces differentiation of ANP-EGFP expressing embryonic stem cells towards a pacemaker phenotype. *FASEB J.* **18**, 1710–1712 (2004).
9. Huber, I. *et al.* Identification and selection of cardiomyocytes during human embryonic stem cell differentiation. *FASEB J.* **21**, 2551–2563 (2007).
10. Klug, M.G., Soonpaa, M.H., Koh, G.Y. & Field, L.J. Genetically selected cardiomyocytes from differentiating embronic stem cells form stable intracardiac grafts. *J. Clin. Invest.* **98**, 216–224 (1996).
11. Laflamme, M.A. *et al.* Cardiomyocytes derived from human embryonic stem cells in pro-survival factors enhance function of infarcted rat hearts. *Nat. Biotechnol.* **25**, 1015–1024 (2007).
12. Xu, C., Police, S., Hassanipour, M. & Gold, J.D. Cardiac bodies: a novel culture method for enrichment of cardiomyocytes derived from human embryonic stem cells. *Stem Cells Dev.* **15**, 631–639 (2006).
13. Monici, M. Cell and tissue autofluorescence research and diagnostic applications. *Biotechnol. Annu. Rev.* **11**, 227–256 (2005).
14. Gropp, M. & Reubinoff, B. Lentiviral vector-mediated gene delivery into human embryonic stem cells. *Methods Enzymol.* **420**, 64–81 (2006).
15. Tsukahara, T. *et al.* Murine leukemia virus vector integration favors promoter regions and regional hot spots in a human T-cell line. *Biochem. Biophys. Res. Commun.* **345**, 1099–1107 (2006).
16. Recchia, A. *et al.* Retroviral vector integration deregulates gene expression but has no consequence on the biology and function of transplanted T cells. *Proc. Natl. Acad. Sci. USA* **103**, 1457–1462 (2006).
17. Woods, N.B. *et al.* Lentiviral vector transduction of NOD/SCID repopulating cells results in multiple vector integrations per transduced cell: risk of insertional mutagenesis. *Blood* **101**, 1284–1289 (2003).
18. van Laake, L.W. *et al.* Human embryonic stem cell-derived cardiomyocytes survive and mature in the mouse heart and transiently improve function after myocardial infarction. *Stem Cell Rev.* **1**, 9–24 (2007).
19. Reinecke, H., Zhang, M., Bartosek, T. & Murry, C.E. Survival, integration, and differentiation of cardiomyocyte grafts: a study in normal and injured rat hearts. *Circulation* **100**, 193–202 (1999).
20. Hattan, N. *et al.* Purified cardiomyocytes from bone marrow mesenchymal stem cells produce stable intracardiac grafts in mice. *Cardiovasc. Res.* **65**, 334–344 (2005).

ONLINE METHODS

Mouse, common marmoset and human PSCs. Mouse ESCs were obtained from Laboratory of Pluripotent Cell Studies, RIKEN Center for Developmental Biology. Common marmoset ESCs (cmESCs) were obtained from Central Institute for Experimental Animals. The human ESC lines (khESC-1, 2 and 3) were obtained from Department of Development and Differentiation, Institute for Frontier Medical Sciences, Kyoto University and were used in conformity with The Guidelines for Derivation and Utilization of Human Embryonic Stem Cells of the Ministry of Education, Culture, Sports, Science and Technology, Japan. Mouse (iPS-MEF-Ng-20D-17) and human (253G4) iPSCs were obtained from Center for iPSC Research and Application, Kyoto University.

Animals. All animals including pregnant and neonatal Wistar rats, and NOD-SCID mice (10 weeks old, male), were purchased from Japan CLEA.

All experimental procedures and protocols were approved by the Animal Care and Use Committees of the Keio University and conformed to the US National Institutes of Health Guide for the Care and Use of Laboratory Animals.

Reagents. MitoTracker dyes (Deep Red, Red, Orange and Green), TMRM, 5,5′,6,6′-tetrachloro-1,1′,3,3′-tetraethylbenzimidazolylcarbocyanine iodide (JC-1), nonyl acridine orange (NAO) and Rhodamine 123 were purchased from Invitrogen. These mitochondria-selective fluorescent dyes can be divided into the Nernstian or non-Nernstian dye groups. The former, including TMRM, can enter into and exit from the mitochondrial matrix freely depending on the mitochondrial membrane potential. In contrast, non-Nernstian dyes such as the MitoTracker dyes cannot exit freely[21]. This characteristic difference may reflect their toxicities and can be used case by case for research, for example, non-Nernstian dyes are used for long-term staining.

The mouse monoclonal antibody to α-actinin (used at 1:400 dilution) was purchased from Sigma-Aldrich. The goat polyclonal antibody to GATA-4 (C-20) and the goat polyclonal antibody for Nkx2.5 (N-19) were purchased from Santa Cruz biotechnology. The mouse monoclonal antibody for SdhB (1:100), Alexa Fluor 488 donkey anti-mouse IgG antibody and Alexa Fluor 546 donkey anti-goat immunoglobulin gamma (IgG) were purchased from Invitrogen.

Maintenance of mouse, marmoset and human PSCs. We maintained mouse ESCs and iPSCs on gelatin-coated dishes in Glasgow Minimum Essential Medium (Sigma) supplemented with 10% FBS (FBS; Equitechbio), 0.1 mM MEM Non-Essential Amino Acids solution (Sigma), 2 mM L-glutamine (Sigma), 0.1 mM β-mercaptoethanol (Sigma) and 2,000 U ml^{-1} mouse LIF (Chemicon). We maintained cmESCs on mouse embryonic fibroblasts in Knockout Dulbecco's Modified Eagle's Medium (KO-DMEM; Invitrogen) supplemented with 20% Knockout Serum Replacement (KSR; Invitrogen), 0.1 mM MEM Non-Essential Amino Acids solution, 2 mM L-glutamine, 0.1 mM β-mercaptoethanol and 4 ng ml^{-1} basic fibroblast growth factor (bFGF; Wako Pure Chemical). We maintained human ESCs and iPSCs similarly to cmESCs, except that Dulbecco's Modified Eagle's Medium/Nutrient Mixture F-12 Ham 1:1 (DMEM-F12; Sigma) was used instead of KO-DMEM.

Differentiation of mouse PSC–derived cardiomyocytes. We performed *in vitro* differentiation of mouse ESCs and iPSCs as described below. We collected mouse PSCs with 0.25% trypsin-EDTA and dissociated them. Seventy-five cells were formed to one embryoid body in one hanging drop with alpha-modified Eagle medium (αMEM; Sigma) supplemented with 10% FBS (Equitechbio). On day 2, we transferred embryoid bodies into floating culture plate with new medium. Four to five days after differentiation, floating embryoid bodies were transferred into attachment culture with nonserum culture medium: αMEM supplemented with insulin-transferrin-selenium (ITS; Sigma). Typically, beating cells appeared on day 7. Embryoid bodies were used for purification experiments between days 12 and 25.

Differentiation of cmESC–derived cardiomyocytes. We performed differentiation of cmESCs as follows. The colonies were detached with 0.1% type three collagenase (Worthington Biochemical) and cultured in cmESC medium lacking bFGF or αMEM and supplemented with 10% FBS (SAFC Biosciences) and 0.1 mM β-mercaptoethanol in bacterial Petri dishes to form embryoid bodies. Typically, 5–20% of embryoid bodies contained beating cells. Embryoid bodies were washed three times with αMEM between days 18 and 25, and cultured with αMEM supplemented with ITS. Embryoid bodies were used for purification experiments between days 30 and 50.

Differentiation of human PSC–derived cardiomyocytes. We grew the detached undifferentiated colonies of human ESCs and iPSCs with αMEM supplemented with 20% FBS (SAFC Biosciences) and 0.1 mM β-mercaptoethanol in bacterial Petri dishes to form embryoid bodies. We observed embryoid bodies containing rhythmically beating cells 16–20 d later. Typically, 1–5% of embryoid bodies contained beating cells. From days 20 to 40, embryoid bodies were washed three times with αMEM and cultured with αMEM supplemented with ITS. Embryoid bodies were used for purification experiments between days 50 and 90.

Staining of cultured embryos. We isolated E11.5 and E12.5 Wistar rat embryos and stained with 50 nM TMRM for 4 h in DMEM with 20% FBS at 30% O_2, 5% CO_2 and 37 °C. Then, we changed to medium without TMRM and incubated the embryos for 4 h to remove unbound dye. We observed the fluorescence signal using conventional fluorescence laser microscopy (IX70 microscope (Olympus) equipped with a color charge-coupled device (CCD) camera (CS220; Olympus)).

Staining *in vivo* embryos. We carried out abdominal surgery on the pregnant Wistar rat on postcoital day 11 under deep anesthesia. We carried out a shallow injection of 100 μl of 500 nM MitoTracker Red solution into the placental side of the exposed ovaries. The rat was sustained under anesthesia for 6 h. Then, under deep anesthesia, we removed the embryos from the rat and observed them using fluorescence microscopy. About 20% of the embryos were positive for MitoTracker Red.

Cardiomyocyte purification. We dispersed the minced hearts, whole rat embryos, or intact embryoid bodies using 0.1% collagenase (Worthington Biochemical), 0.25% trypsin (Becton Dickinson), 20 μg ml^{-1} DNase I (Sigma) and the appropriate

concentration of dyes (10 nM TMRM, 50 nM NAO, 1.5 μM JC-1 or 50 nM MitoTrackers) in Ads buffer (116 mM NaCl, 20 mM HEPES, 12.5 mM NaH_2PO_4, 5.6 mM glucose, 5.4 mM KCl and 0.8 mM $MgSO_4$; pH 7.35) with stirring for 30 min. The dispersed cells were collected and residual cell aggregates were digested again with the same digestion medium. We continued this procedure until all cells were completely dissociated. Finally, all dispersed cells were dissociated with Ads buffer and then analyzed on a FACS (FACS Aria; Becton Dickinson) using 515–545 and 556–601 nm bandpass filters to detect green and red, respectively.

In many cases, nonstained cells exhibited autofluorescence, which may be due to the presence of lipopigments and flavins having broad emission spectrum (450–650 nm)[13]. We suspected that this may affect purity of cardiomyocytes. TMRM can be excited by a 488-nm semiconductor laser and has an emission spectrum that coincides with the red bandpass filter (peak at 575 nm and only 10% of peak fluorescence at 545 nm). Thus, to obtain only cells with high TMRM fluorescence and eliminate contaminating autofluorescent cells, we adopted 'pseudo–two-dimensional separation' in which we observed cells both with red and green filters. In other words, cardiomyocytes received 488 excitation, and then selection for low green and high red fluorescence. Pregating for eliminating doublet fractions, in which one droplet contains more than two cells, was performed according to the manufacturer's instructions.

The TMRM-labeled sorted cells were collected into a tube or were seeded into culture dishes with αMEM containing 10% FBS. For sequential estimation of cardiomyocyte purity, we fixed the sorted cells immediately after collection, then stained them with Nkx2.5 antibody and analyzed again on a FACS. For culture, we used a plate equipped with flexiPERM conA (Greiner Bio-One GmbH) following the manufacturer's instructions. The flexiPERM vessel is a reusable culture funnel, which can adhere tightly onto plastic and glass surfaces. One day after sorting, the flexiPERM vessel was detached from the culture plate and the appropriate amount of medium was added to the plate. This system allowed high-density culture of purified cardiomyocytes in the center of the dish, which enabled good microscopic observation of all cells after detachment of the vessel. For all PSCs, seeded cells were cultured for 5–7 d with αMEM containing 10% FBS, which is necessary for the cells to attach, elongate and develop sarcomere structure, and then fixed and immunofluorescence-stained for α-actinin and Nkx2.5. The culture step is not required for achieving high-purity cardiomyocyte isolation because we have more directly estimated cardiomyocyte purity by sequential FACS analysis.

Transplantation. We purified mouse and human ESC–derived cardiomyocytes, distributed them into nonadhesive 96-well plates (Sumitomo Bakelite) and centrifuged them for 5 min at 100*g*. Two weeks later, the aggregates formed were stained with 50 μM of MitoTracker Red for 2 h in the incubator and washed extensively with Ads buffer. After lightly anesthetizing seven-week-old male NOD-SCID mice with diethylether (Wako Pure Chemical), we intubated them under anesthetization with 1.5% forane (isoflurane, 2-chloro-2-(difluoromethoxy)-1,1,1-trifluoro-ethane) and mechanically ventilated with a Harvard respirator. After this, we performed a left thoracotomy at the third intercostal space and exposed the heart. We inserted a small dead-volume syringe equipped with a 30G needle (Becton Dickinson) containing reaggregated purified cardiomyocytes into the apex, proximally advanced 2–3 mm into the myocardium and released the cells into the myocardium. Then we closed the chest and maintained the mice for 8 weeks before performing a histological examination of these mice.

The 3-(4,5-dimethyl-thiazol-2-yl)-2,5-diphenyltetrazolium bromide (MTT) assay. We treated primary neonatal rat cardiomyocytes with various mitochondrial indicators at 50 nM and 100 nM for 24 h. We added MTT (Wako Pure Chemical) at 0.5 mg ml^{-1} and incubated the cardiomyocytes for 3 h. Then, we dissolved the formazan salt that formed in dimethyl sulfoxide. The absorbance was measured at a wavelength of 550 nm with the background subtracted at 690 nm (SmartSpec3000; Bio-Rad Laboratories). Data were presented as percentage of formazan formation compared to control cells.

Immunofluorescence staining. We fixed cells with 4% paraformaldehyde in phosphate-buffered saline (PBS; pH 7.0) for 20 min. Subsequently, cells were permeabilized with 0.2% Triton X-100 (Sigma) at room temperature (20–28 °C) for 10 min, and then incubated with the primary antibody at 4 °C overnight. Cells were washed with TBS containing 0.1% Tween-20 four times before incubation with the secondary antibodies at room temperature for 30 min. After nuclear staining with DAPI or ToPro-3 (Invitrogen), fluorescence signals were observed using fluorescence microscopy (IX71; Olympus) or confocal laser microscopy (LSM510 META; Carl Zeiss), respectively.

For tissue samples, mice were killed using pentobarbital. The hearts were then perfused from the apex with PBS and fixed by perfusion with 4% paraformaldehyde in PBS (Muto Pure Chemicals). The hearts were then dissected, cryoprotected in sucrose at 4 °C overnight, embedded in OCT compound (Sakura Finetec) and snap-frozen in liquid nitrogen.

Re-aggregation of purified human ESC–derived cardiomyocytes and long-term culture without serum. Human ESC–derived cardiomyocytes were purified and suspended in αMEM supplemented with insulin, transferrin and selenium (ITS) and 0.05% BSA (Invitrogen) in the absence or presence of one of the following growth factors: 25 ng ml^{-1} bFGF (Wako Pure Chemicals); 25 ng ml^{-1} acidic FGF (aFGF); 25 ng ml^{-1} FGF-4; 20 ng ml^{-1} keratinocyte growth factor (KGF); 100 ng ml^{-1} stem cell factor (SCF); 100 ng ml^{-1} vascular endothelial growth factor (VEGF); 10 ng ml^{-1} LIF (Chemicon); 100 ng ml^{-1} glial cell line–derived neurotrophic factor (GDNF); 20 ng ml^{-1} hepatocyte growth factor (HGF); 10 ng ml^{-1} insulin-like growth factor (IGF)-1; 100 ng ml^{-1} epidermal growth factor (EGF); 1×10^{7} M endothelin-1 (ET-1); 10 ng ml^{-1} platelet-derived growth factor (PDGF)-AA; and 100 ng ml^{-1} PDGF-BB. Unless indicated otherwise, growth factors were purchased from R&D Systems Inc. Five hundred cells were distributed into each well ($n = 8$) of cell nonadhesive 96-well plates (MS-0096S; Sumitomo Bakelite) and centrifuged for 5 min at 100*g*.

Total RNA extraction, cDNA synthesis and real-time PCR. Total RNA was prepared from tissues and embryoid bodies using ISOGEN (Nippon gene), according to the manufacturer's instructions. Contaminating genomic DNA was degraded by RNase-free DNase I

doi:10.1038/nmeth.1403

(Ambion) at 37 °C for 30 min. After treatment, DNase I was inactivated by phenol-chloroform extraction and ethanol precipitation. Human heart–derived total RNA was purchased from Takara Bio. We reverse transcribed total RNAs into cDNA using the oligo-(dT)12-18 primer (Superscript II RT kit; Invitrogen). We analyzed the mRNA expression on an ABI 7700 (Applied Biosystems). We listed the target gene name and identification numbers of the primer and probe mixtures (Applied Biosystems) in **Supplementary Table 1**.

21. Jakobs, S. High resolution imaging of live mitochondria. *Biochim. Biophys. Acta.* **1763**, 561–575 (2006).